CONTROL OF CYLINDER WAKE USING A FLEXIBLE FILAMENT

FANGFANG XIE[1], JIAN DENG[1]
[1]*School of Aeronautics and Astronautics,Zhejiang University,*
Hangzhou, Zhejiang, 310027, P.R. China, fangfang_xie@zju.edu.cn

Keywords: *Flexible filaments, suppression, penalty Immersed boundary method*

1 Inroduction

Controlling vortex-induced vibrations (VIV) is important in ocean structures, in designing robust heat exchangers, and especially in the offshore industry given the new emphasis on deep water drilling [1]. In deep water, immersed structures such as risers usually have low damping and over time VIV will weaken the risers and ultimately cause fatigue and fracture. Replacement of the pipelines is a very expensive and time consuming process, hence new suppression techniques are required.

Many flow-control techniques have been proposed to suppress VIV, such as splitter plates [2, 3], suction based flow control [4, 5], slits parallel to the incoming flow [6], stream-lining of the structural geometry [7, 8], helical strakes [9, 10], and other add-on devices for passive control [11, 12, 13]. Recently, flexible plates or filaments have attracted much attention for their role in passive flow control [12, 14], as they can self-adapt to direct flow without the input of energy.

In the current study, control of cylinder wake by using a flexible filament in the downstream stagnation point is numerically studied in the framework of OpenFoam. The cylinder is fixed, and the filament is attached to the base of the cylinder. Its leading end is fixed and its trailing end is free to flap. To execute the numerical simulation and deal with the fluid-structure interaction (FSI) of the filament as well, a penalty Immersed boundary method (IBM) is presented.

2 Numerical method

For the simulations, we adopt a penalty Immersed Boundary Method (IBM)[**?**]. The equations governing this fluid-structure coupling system are expressed as following:

$$\rho\left(\frac{\partial u}{\partial t}+u\cdot\nabla u\right)=-\nabla p+\mu\nabla^2 u+f, \tag{1}$$

$$\nabla\cdot u=0, \tag{2}$$

$$f(x)=\int F(r,s)\delta(x-X(r,s))drds, \tag{3}$$

$$\frac{\partial X}{\partial t}(r,s)=U(r,s)=\int u(x,t)\delta(x-X(r,s))dx, \tag{4}$$

$$F=F_E+F_K+F_C, \tag{5}$$

$$F_E=-\frac{\partial E}{\partial X}, \tag{6}$$

$$F_K(r,s)=K[Y(r,s)-X(r,s)], \tag{7}$$

$$F_C(r,s)=\delta(X(r,s)-X'(s))\frac{X-X'}{|X-X'|}, \tag{8}$$

$$\rho_s(r,s)\frac{\partial^2 Y}{\partial^2 t}=-F_K(r,s)-\rho_s(r,s)Fr\frac{\mathbf{g}}{g}. \tag{9}$$

Equations 1 and 2 are the Navier-Stokes equations for a viscous incompressible fluid, which are solved by a finite-volume based solver OpenFOAM. Here, ρ, u, p are the density, velocity and pressure of the fluid, respectively. The term $F(r,s)$ in equation 3 include the elastic force induced by the deformation of the elastic boundary and the repulsive force between the filament and cylinder, and the term $f(x)$ represents the fluid body force density.

For the rigid cylinder, the F_E component can be ignored. For the flexible filament, it can be regarded as a 1-D massive boundaries, which are represented by a serial of one-dimensional rods. We impose two elasticities to these rods, one resists stretching and compression, and the other resists bending. The energy function $E[X(.)]$ can therefore be formalized as

$$E[\mathbf{X}(\cdot)] = \frac{1}{2}k_s \int \left(\left|\frac{\partial X}{\partial s}\right| - 1\right)^2 ds + \frac{1}{2}k_b \int \left|\frac{\partial^2 X}{\partial^2 s}\right|^2 ds, \tag{10}$$

where k_s and k_b denote the coefficients by resisting the stretching and bending respectively.

3 Numerical results

In the current work, we consider a fixed Reynolds number, Re = 100, for the following simulations. We define the Reynolds number $Re = U_\infty/\nu D$, where D is the diameter of the circular cylinder, U_∞ is the streamwise velocity far upstream and ν is the kinematic viscosity.

We firstly examine the effects of the filament on the flow control of the cylinder by varying the length (L) of the filament. Figure 1 shows the phase diagram of drag and lift coefficients for the cylinder-filament system under various length. The black line denotes the reference value for the cylinder without filaments. It is seen that the effect of the attached filament on the evolution of the forces acting on the cylinder is remarkable. With the attached filament, both the mean drag coefficient and the fluctuation of lift force can be suppressed effectively. The longer filament performs better since it can delay the vortex shedding in the cylinder wake to a further downstream, see figure 2.

For the case with the filament length of $L = 0.5D$ and $L = D$, the symmetry of lift fluctuation is broken and a positive net lift force is achieved. By looking at the flapping trajectory of the filament in figure 3, we see that the filament is flapping in the low half part of the cylinder wake, thus generating a positive lift force to the cylinder-filament system.

Moreover, as the effect of the bending stiffness, we see that in figure 4 a more rigid filament can achieve a lower drag coefficient and smaller lift fluctuation/ flapping amplitude . By checking the flow pattern, it is seen that the vortex is roll up back to the top surface of the filament tail for the rigid one (with $kb = 0.002$), therefore leading to the recovery of pressure in the wake of filament.

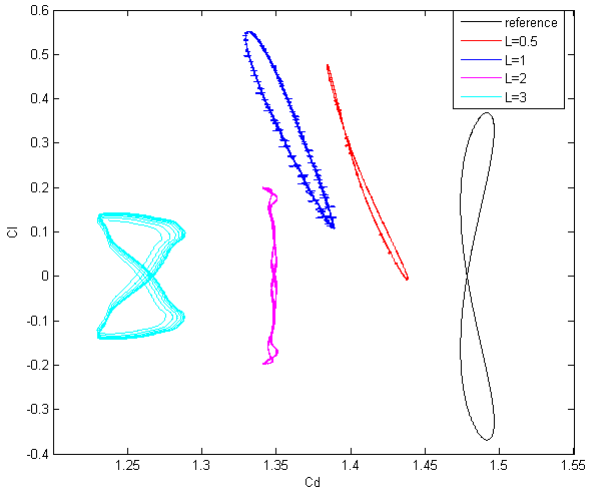

Figure 1: Effect of filament's length on the force of the cylinder-filament system.

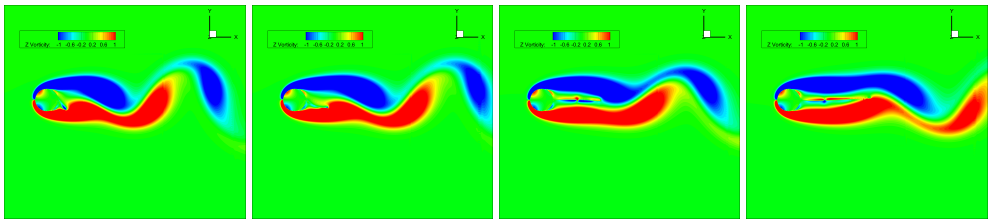

Figure 2: Vorticity plot for flow around a cylinder with a single filament attached to the downstream stagnation point under various length ($\rho_s = 1, kb = 0.01$).

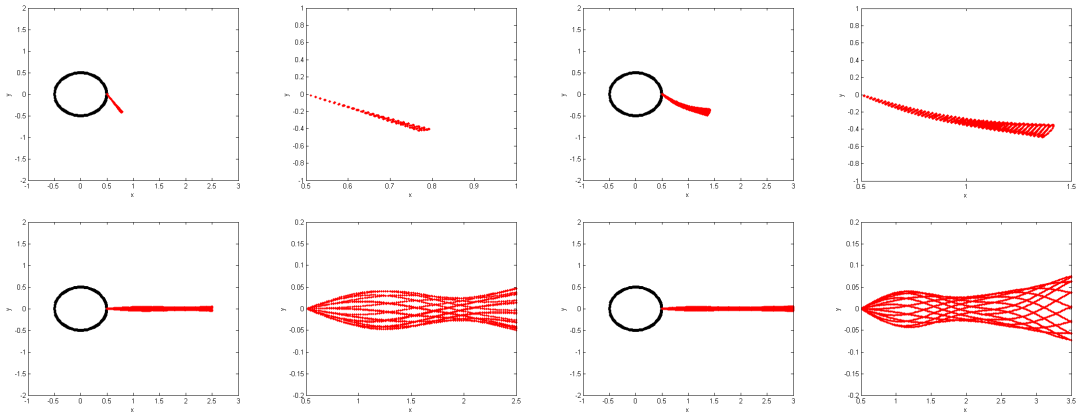

Figure 3: Ranges of motion of the filament attached on the cylinder under various length ($\rho_s = 1, kb = 0.01$).

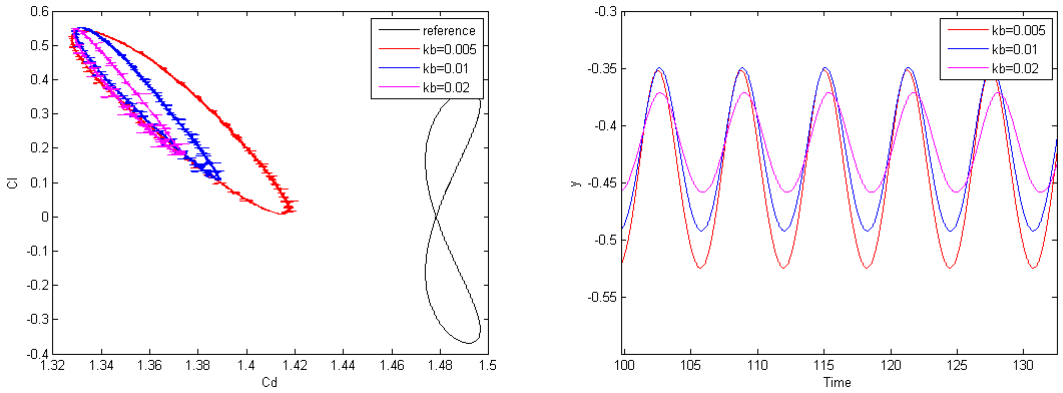

Figure 4: Effect of bending stiffness on the force and tail displacement of the cylinder-filament system.

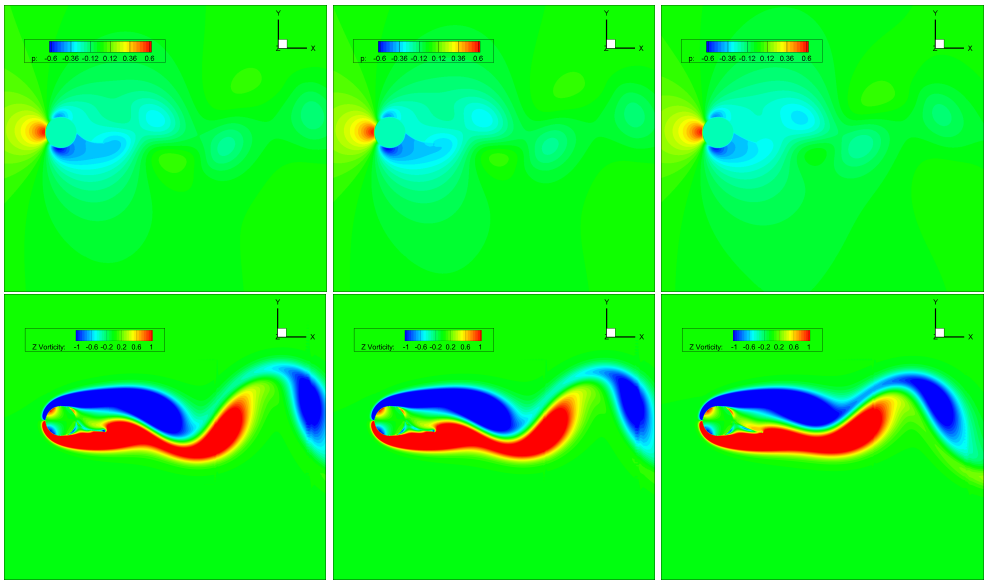

Figure 5: Effect of bending stiffness on the flow pattern of the cylinder-filament system.Left Column: $kb = 0.0005$, Middle Column:$kb = 0.001$, Right Column: $kb = 0.002$. Top row: pressure contour, bottom row: vorticity contour.

Acknowledgments

The authors gratefully acknowledges the support by the National Natural Science Foundation of China (Grant No. 11602217).

References

[1] C. H. K. Williamson and R. Govardhan, "Vortex-induced vibrations," *Annu. Rev. Fluid Mech.*, vol. 36, pp. 413–455, 2004.

[2] G. R. S. Assi, P. W. Bearman, and N. Kitney, "Low drag solutions for suppressing vortex-induced vibration of circular cylinders," *Journal of Fluids and Structures*, vol. 25, no. 4, pp. 666–675, 2009.

[3] Y. Bao and J. Tao, "The passive control of wake flow behind a circular cylinder by parallel dual plates," *Journal of Fluids and Structures*, vol. 37, pp. 201–219, 2013.

[4] S. Dong, G. S. Triantafyllou, and G. E. Karniadakis, "Elimination of vortex streets in bluff-body flows," *Physical review letters*, vol. 100, no. 20, p. 204501, 2008.

[5] W. Chen, D. Xin, F. Xu, H. Li, J. Ou, and H. Hu, "Suppression of vortex-induced vibration of a circular cylinder using suction-based flow control," *Journal of Fluids and Structures*, vol. 42, pp. 25–39, 2013.

[6] H. Baek and G. E. Karniadakis, "Suppressing vortex-induced vibrations via passive means," *Journal of Fluids and Structures*, vol. 25, no. 5, pp. 848–866, 2009.

[7] J. P. Pontaza and R. G. Menon, "Numerical simulations of flow past an aspirated fairing with three degree-of-freedom motion," in *ASME 2008 27th International Conference on Offshore Mechanics and Arctic Engineering*. American Society of Mechanical Engineers, 2008, pp. 799–807.

[8] D. Corson, S. Cosgrove, and Y. Constantinides, "Application of CFD to predict the hydrodynamic performance of offshore fairing designs," in *ASME 2014 33rd International Conference on Ocean, Offshore and Arctic Engineering*. American Society of Mechanical Engineers, 2014, pp. V002T08A079–V002T08A079.

[9] D. W. Allen, D. L. Henning, J. H. Haws, D. W. McMillan, and R. B. McDaniel, "Partial helical strake for vortex-induced-vibrationsuppression," May 13 2003, uS Patent 6,561,734.

[10] A. D. Trim, H. Braaten, H. Lie, and M. A. Tognarelli, "Experimental investigation of vortex-induced vibration of long marine risers," *Journal of fluids and structures*, vol. 21, no. 3, pp. 335–361, 2005.

[11] J. C. Owen, P. W. Bearman, and A. A. Szewczyk, "Passive control of VIV with drag reduction," *Journal of Fluids and Structures*, vol. 15, no. 3, pp. 597–605, 2001.

[12] J. Wu, Y. Qiu, C. Shu, and N. Zhao, "Flow control of a circular cylinder by using an attached flexible filament," *Physics of Fluids*, vol. 26, no. 10, p. 103601, 2014.

[13] F. Xie, Y. Yu, Y. Constantinides, M. S. Triantafyllou, and G. E. Karniadakis, "U-shaped fairings suppress vortex-induced vibrations for cylinders in cross-flow," *Journal of Fluid Mechanics*, vol. 782, pp. 300–332, 2015.

[14] J. Favier, A. Dauptain, D. Basso, and A. Bottaro, "Passive separation control using a self-adaptive hairy coating," *Journal of Fluid Mechanics*, vol. 627, pp. 451–483, 2009.